Loss-of-Function Mutation in Thiamine Transporter 1 in a Family With Autosomal Dominant Diabetes

Prapaporn Jungtrakoon,[1,2,3] Jun Shirakawa,[1,4] Patinut Buranasupkajorn,[1,2,5] Manoj K. Gupta,[1,4] Dario F. De Jesus,[1,4] Marcus G. Pezzolesi,[6] Aussara Panya,[1,2,3] Timothy Hastings,[2] Chutima Chanprasert,[3] Christine Mendonca,[2] Rohit N. Kulkarni,[1,4] and Alessandro Doria[1,2]

Diabetes 2019;68:1084–1093 | https://doi.org/10.2337/db17-0821

Solute Carrier Family 19 Member 2 (*SLC19A2*) encodes thiamine transporter 1 (THTR1), which facilitates thiamine transport across the cell membrane. *SLC19A2* homozygous mutations have been described as a cause of thiamine-responsive megaloblastic anemia (TRMA), an autosomal recessive syndrome characterized by megaloblastic anemia, diabetes, and sensorineural deafness. Here we describe a loss-of-function *SLC19A2* mutation (c.A1063C: p.Lys355Gln) in a family with early-onset diabetes and mild TRMA traits transmitted in an autosomal dominant fashion. We show that *SLC19A2*-deficient β-cells are characterized by impaired thiamine uptake, which is not rescued by overexpression of the p.Lys355Gln mutant protein. We further demonstrate that *SLC19A2* deficit causes impaired insulin secretion in conjunction with mitochondrial dysfunction, loss of protection against oxidative stress, and cell cycle arrest. These findings link *SLC19A2* mutations to autosomal dominant diabetes and suggest a role of *SLC19A2* in β-cell function and survival.

SLC19A2 encodes thiamine transporter 1 (THTR1), a transmembrane protein that facilitates the transport of thiamine by shielding its positive charge from the repulsive force of the membrane. Homozygous *SLC19A2* mutations have been described as the cause of thiamine-responsive megaloblastic anemia (TRMA) (Online Mendelian Inheritance in Man [OMIM] #249270), a syndrome characterized by megaloblastic anemia, diabetes, sensorineural deafness (1), and the variable combination of other neurological, cardiovascular, and neuroendocrine abnormalities such as optic atrophy (2), arrhythmia, heart defects (3,4), thyroid function alterations (5), and seizures (6).

Thiamine, also known as vitamin B1, acts as coenzyme of the cytosolic enzyme transketolase (TKT), which is part of the pentose phosphate pathway (PPP) responsible for the generation of NADPH and ribose-5-phosphate—a precursor of high-energy ribonucleotides (e.g., ATP) and nucleotides. Thiamine is also the coenzyme for several mitochondrial enzymes, including pyruvate dehydrogenase (PDH), α-ketoglutarate dehydrogenase (α-KGDH), branched-chain α-ketoglutarate dehydrogenase (BCKD), and 2-hydroxyphytanoyl-CoA lyase. The megaloblastic anemia associated with *SLC19A2* mutations appears to be due to impaired TKT activity, which, by reducing the availability of nucleotides, causes red cell precursors to continue to grow in size without dividing. The coexistence of sensorineural deafness and the other neurological and cardiovascular abnormalities found in the TRMA syndrome are suggestive of an underlying mitochondrial dysfunction, which might be due, in part, to impaired PDH (7) and α-KGDH (8) activities causing defective energy production, to which tissues with a high demand for energy, such as the auditory, visual, cardiovascular, and central nervous systems, are particularly sensitive (9–11).

The form of diabetes that is part of the TRMA syndrome is nonautoimmune and is characterized by an insulin secretion deficit and a time of onset ranging from birth to adolescence. Insulin treatment is usually needed, although the insulin requirement may be reduced in some cases by

[1]Department of Medicine, Harvard Medical School, Boston, MA
[2]Section on Genetics and Epidemiology, Joslin Diabetes Center, Boston, MA
[3]Section on Islet Cell and Regenerative Biology, Joslin Diabetes Center, Boston, MA
[4]Division of Molecular Medicine, Research Department, Faculty of Medicine, Siriraj Hospital, Mahidol University, Bangkok, Thailand
[5]Division of Hospital and Ambulatory Medicine, Department of Medicine, Faculty of Medicine, Chulalongkorn University, Bangkok, Thailand
[6]Division of Nephrology and Hypertension, University of Utah School of Medicine, Salt Lake City, UT

Corresponding author: Alessandro Doria, alessandro.doria@joslin.harvard.edu

Received 12 July 2017 and accepted 23 February 2019

This article contains Supplementary Data online at http://diabetes.diabetesjournals.org/lookup/suppl/doi:10.2337/db17-0821/-/DC1.

high-dose thiamine supplementation (12,13). The TRMA syndrome has been reported in >50 families worldwide (14). While in most cases heterozygous *SLC19A2* mutation carriers have not been described as having diabetes, adult-onset glucose intolerance with or without a hearing defect was reported among these subjects in three TRMA kindreds (15). The question as to whether a single allele defect of *SLC19A2* may cause diabetes has never been addressed. In this study, we report a loss-of-function mutation in the *SLC19A2* gene linked, albeit with incomplete penetrance, to autosomal dominant diabetes with mild TRMA clinical signs and show suggestive evidence for *SLC19A2* deficiency causing impaired insulin secretion and diabetes by determining mitochondrial dysfunction, loss of protection against oxidative stress, and cell cycle arrest in β-cells.

RESEARCH DESIGN AND METHODS

Whole-Exome Sequencing

Fifty-two extended families with autosomal dominant diabetes underwent whole-exome sequencing as reported by Prudente et al. (16). Variants were filtered as previously described. Briefly, variants that were heterozygous, were reported in public databases (dbSNP142, 1000 Genomes, and Exome Variant Server [EVS]) with frequency <0.01, were shared by affected family members, and were potentially deleterious as determined by a panel of prediction softwares were included in the analysis (16). In the former study, the focus was on variants that were located in genes with functional relevance to glucose metabolism as determined by an analysis with GeneDistiller (16). In the current study, we reanalyzed those same exome sequencing data focusing on variants placed in a second set of candidate genes, namely, genes that are mutated in rare forms of syndromic diabetes. These included the *WFS1*, *CISD2*, *ALMS1*, and *SLC19A2* genes, which are mutated in Wolfram type 1, Wolfram type 2, Alström, and TRMA syndromes, respectively. Filtered variants were validated and analyzed for segregation with diabetes in the families by means of Sanger DNA sequencing. Variants were considered to segregate with diabetes if ≥80% of carriers >40 years old had developed diabetes and there were no phenocopies whose phenotype was not consistent with either type 1 or older-onset type 2 diabetes.

Cell Culture

The mouse insulinoma cell line MIN6-m9 (17) was kindly provided by Prof. S. Seino, Kobe University. Unless indicated otherwise, cells (passages 27–40) were maintained in DMEM (Corning) containing 4 mmol/L L-glutamine, 25 mmol/L glucose, and 0.01 mmol/L thiamine, supplemented with 10% FBS (BenchMark), 0.1 mg/mL streptomycin, and 100 units/mL penicillin (Corning) at 37°C and with 5% CO_2 humidified condition.

Human and Mouse Islets

Human islets were obtained from the Integrated Islet Distribution Program. All studies and protocols were approved by the Joslin Diabetes Center's Committee on Human Studies (CHS#5-05). Upon receipt, islets were cultured overnight in Miami Media #1A (Cellgro). Mouse islets were isolated from wild-type C57BL/6 mice. Islets were handpicked and cultured overnight in RPMI media containing 5 mmol/L glucose and 10% FBS. For immunostaining studies, islets were embedded in agarose and used. For insulin secretion studies, islets were starved in Final Wash/Culture Media (Cellgro) for 5 h before being stimulated with 10 nmol/L insulin.

Immunohistochemistry and Immunoblotting

Human and mouse islets were analyzed by immunostaining using anti-THTR1 (sc-27656; Santa Cruz Biotechnology) and anti-insulin (ab7842; Abcam). Images were taken with an LSM7 confocal laser scanning microscope (Carl Zeiss). For immunoblotting, MIN6-m9 cells, mouse islets, or human islets were solubilized in M-PER lysis buffer (Thermo Scientific) with protease inhibitors and phosphatase inhibitors (Sigma-Aldrich), and protein concentration was measured using a BCA protein assay kit (Pierce). Extracts were subjected to Western blotting with primary antibodies overnight at 4°C. Mouse and human anti-THTR1, anti–β-actin, and anti–α-tubulin antibodies were from Sigma-Aldrich (HPA016599), Cell Signaling Technology (4970), and Abcam (ab7291), respectively.

Cellular Localization of SLC19A2-GFP Fusion Proteins

The coding sequence of the human *SLC19A2* gene (NM_006996; OHu18269C [GenScript]) was subcloned into the pAcGFP1-N1 vector (Addgene) at *Xho*I and *Age*I sites. The SLC19A2-WT-GFP (GFP-tagged wild type [WT]) construct was used as a template for generation of SLC19A2-K355Q-GFP (GFP-tagged mutant) by means of site-directed mutagenesis using the Q5 Site-Directed Mutagenesis Kit (NEB). Primers for cloning and mutagenesis are provided in Supplementary Table 1. Plasmid constructs were transiently transfected into MIN6-m9 using METAFECTENE PRO (Biontex). Twenty-four hours after transfection, cells were trypsinized and transferred to poly-L-lysine–coated glass-bottom dishes. Live cell imaging was performed at 72 h after transfection with an LSM7 confocal laser scanning microscope (Carl Zeiss).

SLC19A2 Suppression and Quantitative RT-PCR Analysis

Lentiviral transduction particles (Sigma-Aldrich) carrying shRNAs (TRCN0000324923) (knockdown [KD]23) targeting the common part of the long and short isofoms of mouse *SLC19A2* (NM_054087 and NM_001276455) and nonmammalian shRNA control particles (nontargeted control [NTC]) (Sigma-Aldrich) were added to cultured MIN6-m9 on day 1 followed by 3 μg/mL puromycin selection for 10 days. Total RNA was extracted from cells using the RNeasy Mini Kit (QIAGEN). Reverse transcription and quantitative PCR were performed using the SuperScript III Platinum SYBR Green One-Step qRT-PCR Kit (Life

Technologies) on an ABI 2900HT thermocycler with gene-specific primers for the long SLC19A2 isoform (Supplementary Table 1). Results were normalized to mouse TATA box binding protein (*TBP*) expression levels.

Analysis of Thiamine Uptake

Thiamine uptake was measured at 48 h after transfection. Cells were washed and preincubated for 15 mins at 37°C in Krebs-Ringer buffer (in mmol/L: 133 NaCl, 4.93 KCl, 1.23 $MgSO_4$, 0.85 $CaCl_2$, 5 glucose, 5 glutamine, 10 HEPES, and 10 MES; pH 8.0). Thiamine[3H(G)] hydrochloride (American Radiolabeled Chemical, Inc.), with or without unlabeled thiamine hydrochloride (Sigma-Aldrich), was added to preincubated cells to obtain a final concentration of 15 nmol/L and 1 mmol/L of labeled and unlabeled thiamine, respectively. The reaction was terminated after 5 min by adding ice-cold buffer followed by immediate aspiration. Cells were washed three times with ice-cold buffer and lysed with M-PER lysis buffer. Lysate radioactivity was measured using a scintillation analyzer (Packard). Specific uptake was calculated by subtracting the radioactivity incorporated in the presence of unlabeled thiamine from the radioactivity incorporated in the absence of an unlabeled competitor. Uptake data were normalized by protein content.

Extracellular Flux Analysis

Cells were suspended in DMEM containing 5.5 mmol/L glucose and seeded onto Seahorse XF24 Cell Culture Microplates at a density of 50,000 cells/well. Oxygen consumption rate and extracellular acidification rate were measured by means of extracellular flux analysis with the Seahorse instrument (Seahorse Bioscience) at 18–24 h after seeding. Basal respiration was measured for ~100 min. Glucose (25 mmol/L), oligomycin (2 μmol/L), FCCP (4 μmol/L), and rotenone plus actinomycin A (0.2 μmol/L each) were added at approximately 15, 35, 55, and 75 min, respectively.

Glucose-Stimulated Insulin Secretion

Cells were washed twice with PBS and preincubated in Krebs-Ringer bicarbonate (KRB) buffer with 2.8 mmol/L glucose for 2 h. Preincubation buffer was replaced with 2.8 mmol/L glucose in KRB for 1 h, followed by 16.7 mmol/L glucose in KRB for 1 h. Insulin release was measured by means of ELISA (Crystal Chem).

Analysis of Cell Proliferation

A total of 250,000 MIN6-m9 cells were seeded onto poly-L-lysine–coated coverslips. Eighteen hours later, the cell proliferation rate was determined by means of the EdU incorporation assay. The number of EdU-positive cells was determined among at least 1,000 immunostained nuclei per coverslip using an LSM7 confocal laser scanning microscope. Three coverslips per condition were assayed in triplicate for each individual experiment.

Analysis of Oxidative Stress–Induced Apoptosis

A total of 250,000 MIN6-m9 cells were seeded per well in a 12-well plate 24 h before H_2O_2 treatment. Cells were then cultured in FBS-free DMEM, with or without 20 μmol/L H_2O_2 (18), for another 18–24 h. Apoptosis was measured by Annexin V and 7-ADD staining using the PE Annexin V Apoptosis Detection Kit I (BD Bioscience), and processed for flow cytometry (LSR II; BD Bioscience).

Statistics

All assays were performed at least three times. Results are shown as means ± SE. Data were analyzed by means of mixed effect linear regression with the exposure/treatment of interest (knockdown [KD] vs. scramble) as a fixed effect and the variable "experiment" (i.e., the specific occasion when an experiment was performed) as a random effect to account for day-to-day variability in reagents and other experimental conditions. Analyses were carried out using SAS software, version 9.4. Differences were considered significant at $P < 0.05$.

Data and Resource Availability

The data sets generated during and/or analyzed during the current study are available from the corresponding author upon request.

RESULTS

An *SLC19A2* Mutation in a Family With Autosomal Dominant Diabetes and Mild TRMA Traits

By browsing existing exome sequencing data from 52 families with autosomal dominant diabetes (16), we identified six variants in three genes known to be mutated in syndromic forms of diabetes (Supplementary Table 2). One of the six variants—a missense mutation in the *SLC19A2* gene (NM_006996: c.A1063C: p.Lys355Gln)—segregated with diabetes in the family in which it was found (kindred F23) (Fig. 1*A*). Homozygous *SLC19A2* mutations have been described as a cause of the autosomal recessive TRMA syndrome. However, variant p.Lys355Gln was found in heterozygosis, rather than homozygosis, in all five members with diabetes of kindred F23 as well as in a member without diabetes who was 40 years old at the time of examination (Fig. 1*B*). Diabetes was diagnosed at an age ranging from 2 to 35 years and was treated with insulin in all but one case. Three of the four insulin-treated subjects had measurable fasting C-peptide (this information was not available for the remaining subject) (Table 1). Four of the mutation carriers had normal BMI, and two were overweight (Table 1). In addition to diabetes, mutation carriers reported a variety of health problems that could be viewed as related to the TRMA syndrome, such as unspecified thyroid dysfunction, cardiac arrhythmia, and seizures. Of note, the family member who was nonpenetrant with regard to diabetes (subject II-4) reported a history of cardiac arrhythmia. None of the family members were reported to be deaf, although their auditory acuity had not been

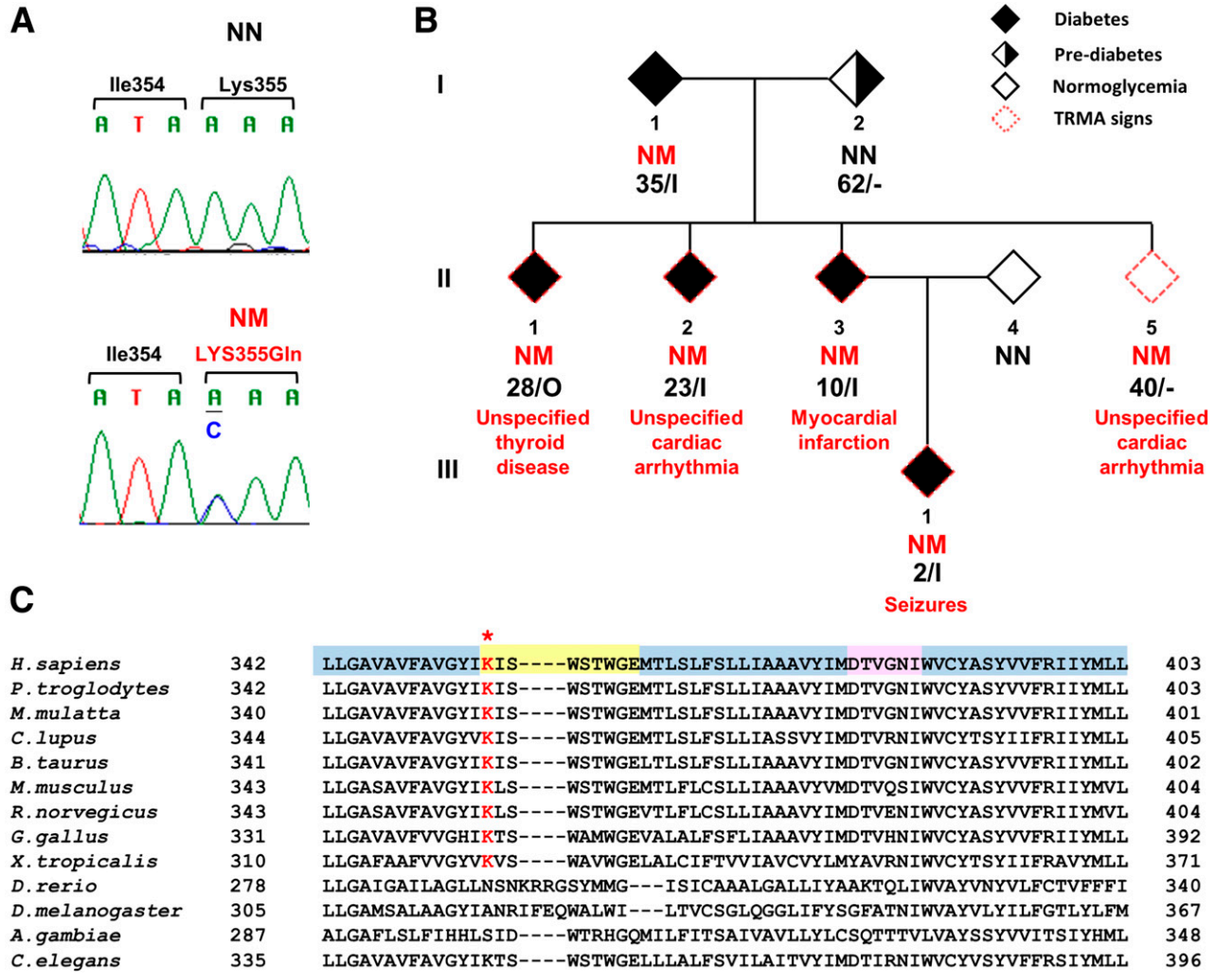

Figure 1—*SLC19A2* mutation in a family with autosomal dominant diabetes. *A*: Sequence chromatograms showing heterozygosis for the *SLC19A2* p.Lys355Gln mutation. Primer sequences for amplification of the genomic region flanking the p.Lys355Gln mutation and for Sanger sequencing are provided in Supplementary Table 5. *B*: Pedigree structure of the family with the *SLC19A2* p.Lys355Gln mutation. Filled and open symbols represent individuals with diabetes and individuals without diabetes, respectively; half-filled symbol represents individuals with prediabetes, and symbols with a red dash border represent individuals with clinical features related to TRMA. NM indicates presence of the p.Lys355Gln mutation; NN indicates absence of the mutation. The age at examination or the age at diagnosis is shown along with the current treatment under the genotypes; I, insulin; O, oral hypoglycemic agents. *C*: Multiple amino acid alignments of THTR1 across species. The asterisk indicates the mutated amino acid. Residues residing in transmembrane, cytosolic, and extracellular domains are highlighted in blue, yellow, and pink, respectively.

measured. Data concerning red cell number and/or morphology were not available. In addition to the described *SLC19A2* mutation, five other mutations were identified in this family in genes that had not been selected by GeneDistiller in the previous report (16) and were not known to be mutated in syndromic or neonatal diabetes (Supplementary Table 3). One of these mutations (NM_001193302: c.A4G: p.I2V), residing in the *SEMA4A* (semaphorin 4A) gene, showed the same pattern of segregation with diabetes as *SLC19A2* p.Lys355Gln. However, considering the link between SLC19A2 and TRMA syndrome and the TRMA-like symptoms in the family, we focused further functional studies on the *SLC19A2* mutation.

Loss of THTR1 Function Caused by the p.Lys355Gln Mutation

THTR1, the thiamine transporter 1 coded by *SLC19A2*, consists of 12 transmembrane domains. Lys355 is the first cytoplasmic residue after transmembrane domain 8 and is highly conserved among species (including rat and mouse) with a phyloP score of 0.99 (Fig. 1*C*). The mutation was previously reported in public databases as rs200879349, with a frequency of 0.004% (5 out of 121,098 exomes in the Exome Aggregation Consortium database). Four out of five sequence-based prediction tools suggested a deleterious effect of the 355Gln substitution (Supplementary Table 4). Also, while the THTR1 crystal structure is not available, the MUpro software, which analyzes the effect of

Table 1—Clinical and genetic characteristics of examined members from the family with the SLC19A2 heterozygous mutation

ID	Mutation	Sex	Age (years)	Age at diagnosis (years)	BMI (kg/m^2)	DM status	Current treatment	FPG (mg/dL)	PG 2 h after OGTT (mg/dL)	HbA_{1c} (%)	HbA_{1c} (mmol/mol)	Fasting insulin (μIU/mL)	Insulin 2 h after OGTT (μIU/mL)	Fasting C-peptide (ng/mL)	TRMA clinical sign
I-1	Yes	M	66	35	25.41	DM	Insulin	NA	NA	6.6	49	NA	NA	0.24	—
I-2	No	F	62	62	26.88	PD	None	97	161	6.2	44	14	141.6	NA	—
II-1	Yes	F	38	28	24.83	DM	OHA	NA	NA	8.5	69	12.1	NA	NA	Unspecified thyroid disease
II-2	Yes	F	36	23	26.88	DM	Insulin	NA	NA	8.3	67	NA	NA	0.53	Unspecified cardiac arrhythmia
II-3	Yes	F	33	10	21.35	DM	Insulin	183	NA	10.4	90	NA	NA	0.57	Myocardial infraction
II-5	Yes	F	40	—	19.77	NG	None	107	47	4.9	30	4.2	2.7	NA	Unspecified cardiac arrhythmia
III-1	Yes	F	5	2	16.02	DM	Insulin	295	NA	7.2	55	NA	NA	NA	Seizures

DM, diabetes mellitus; F, female; FPG, fasting plasma glucose; HbA_{1c}, glycated hemoglobin; M, male; NA, not available; NG, normal glucose; OGTT, oral glucose tolerance test; OHA, oral antidiabetes agents; PD, prediabetes (as indicated by $HbA_{1c} \geq 5.7\%$, according to American Diabetes Association criteria); PG, plasma glucose.

amino acid substitutions based on the primary sequence, predicted a decrease in stability of protein structure in response to this mutation (Supplementary Table 4). To obtain further insights into the functional role of *SLC19A2* in pancreatic β-cells, we investigated *SLC19A2* expression in primary human (Fig. 2*A* and *B*) and mouse (Fig. 2*C* and *D*) islets by means of immunohistochemistry and Western blot analysis. *SLC19A2* was expressed in both insulin-positive β-cells and insulin-negative non-β-cells in the islets of both humans (Fig. 2*A*) and mice (Fig. 2*C*). Immunostaining also revealed expression of *SLC19A2* in a human β-cell line (Fig. 2*E*). Its expression was not modulated by insulin (Fig. 2*B*). In a previous study of mouse pancreatic β-TC-6 cells (19), TRMA mutations were shown to determine a cytosolic localization of mutant THTR1 as opposed to the predominant plasma membrane localization of the wild-type protein. The intracellular localization of the mutant transporter was paralleled by an impairment of thiamine uptake. To investigate whether the same was true for p.Lys355Gln, plasmid constructs for the expression of GFP-tagged wild-type (WT-GFP) and mutant (K355Q-GFP) human *SLC19A2* were transiently expressed in the mouse insulinoma cell line MIN6-m9. As previously observed with other *SLC19A2* mutations, K355Q-GFP was preferentially localized in the cytoplasm, with a vesicle-like pattern, whereas the WT-GFP predominantly targeted the cell surface (Fig. 3*A*). This finding suggested mislocalization of the mutant protein, which was possibly caused by protein misfolding related to the structural instability predicted by the MUpro software. Although mRNA levels were similar (Supplementary Fig. 1*A*), protein levels of THTR1-K355Q appeared to be higher than that of THTR1-WT (Supplementary Fig. 1*B* and *C*), suggesting resistance of THTR1-K355Q to protein quality control mechanisms.

To further test the functional impact of the mutation, stable *SLC19A2*-KD MIN6-m9 cells were generated using lentiviral particles delivering two different shRNAs (KD23 and KD28). Compared with the NTC, the KD23 clone showed the highest KD efficiency, resulting in 68% and 46% reduction in *SLC19A2* mRNA and protein levels, respectively (Fig. 3*B* and *C*). Expression of the *SLC19A3* gene, coding for another thiamine transporter (THTR2), increased in response to the *SLC19A2* KD (Table 2). However, despite this, the ability of the KD23 MIN6-m9 clone in taking up [^{3}H]thiamine was significantly impaired (−36%) compared with the NTC cells (Fig. 3*D*). The defective thiamine uptake was normalized by transient expression of WT-GFP but not K355Q-GFP, confirming the loss of function of the K355Q mutant THTR1 (Fig. 3*E*).

Impact of THTR1 Deficiency on β-Cells

Mutations in mitochondrial DNA cause a form of diabetes that is associated with sensorineural deafness, retinal abnormalities, and muscular involvement (20,21)—a clinical picture similar to that of diabetes associated with the

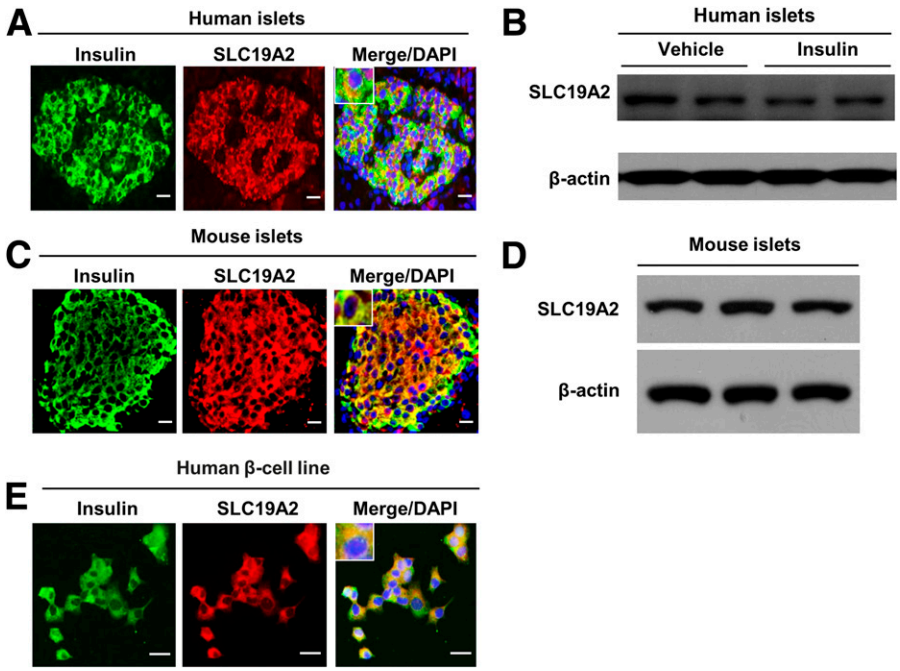

Figure 2—SLC19A2 expression in human and mouse islets. Representative immunostaining for insulin (green), SLC19A2 (red), and nucleus (blue) and Western blot analysis of endocrine pancreas (n = 3). Immunostaining for SLC19A2 and insulin (*A*) and Western blot analysis of SLC19A2 in human islets (*B*). Immunostaining for SLC19A2 and insulin (*C*) and Western blot analysis of SLC19A2 in mouse islets (*D*). *D*: Immunostaining for SLC19A2 and insulin in human β-cell line. Scale bars = 20 μm.

TRMA syndrome (1,7). Since thiamine is the coenzyme for PDH and α-KGDH, which are critical enzymes for energy production by mitochondria, we hypothesized that *SLC19A2* mutations may cause diabetes by causing mitochondrial dysfunction. To test this hypothesis, we compared the profiles of mitochondrial respiration in KD23 MIN6-m9 and NTC cells by means of extracellular flux analysis. Basal respiration, ATP synthesis, and non-mitochondrial respiration were significantly reduced in KD23 MIN6-m9 compared with NTCs (Fig. 4*A*). These alterations were closely mirrored by significantly lower insulin secretion responses to glucose in KD23 MIN6-m9 (Fig. 4*B*). The glycolytic activity, as determined by the extracellular acidification rate, was decreased but not significantly different in KD23 MIN6-m9 compared with NTC (Supplementary Fig. 2). As mentioned above, thiamine is also the coenzyme of TKT, which plays a critical in the production of ribose-5-phosphate, NADPH, ATP, nucleic acids, and glutathione through the pentose phosphate pathway. Thus, thiamine is not only necessary to maintain ATP production but is also required for DNA duplication (22,23) and for detoxification (22,24,25). To test the hypothesis that THTR1 deficiency may lead to cell cycle arrest and apoptosis of β-cells, we investigated rates of proliferation and oxidative stress–induced apoptosis in *SLC19A2*-defective MIN6-m9 cells. Although previous studies of *SLC19A2* $^{-/-}$ mice did not show a reduction of β-cell mass (26), we observed a 30% decrease in cell proliferation rate and a twice-as-large hydrogen peroxide–induced increase in apoptosis in KD23 MIN6-m9 compared with NTC cells (Fig. 4*C* and *D*). The lack of an apparent change in β-cell mass in the *SLC19A2* $^{-/-}$ mice could be due to secondary factors that can regulate β-cell mass in vivo that are not operative in vitro (KD23 in MIN6 cells). Further work is necessary to directly address the regulatory effects on β-cell mass.

Expression of *SLC19A2* in β-Cells From Subjects With Diabetes and *db/db* Mice

To obtain additional information about the relationship between *SLC19A2* and glucose homeostasis, we investigated *SLC19A2* expression levels in the islets of patients with common, multifactorial forms of type 2 diabetes (Supplementary Table 5). Although not statistically significant, we observed a trend (P = 0.08) for lower *SLC19A2* mRNA levels in islets from patients with type 2 diabetes compared with islets from control subjects without diabetes (Supplementary Fig. 3). We also observed a marked reduction of cells stained with both anti-insulin and anti-THTR1 antibodies in the pancreas of obese *db/db* mice compared with db/+ mice (Supplementary Fig. 4).

DISCUSSION

Homozygous mutations in the *SLC19A2* gene, coding for thiamine transporter THTR1, are known to cause the TRMA syndrome, characterized by diabetes, anemia, sensorineural deafness, and other clinical abnormalities (1). In this report, we show that the occurrence of a single

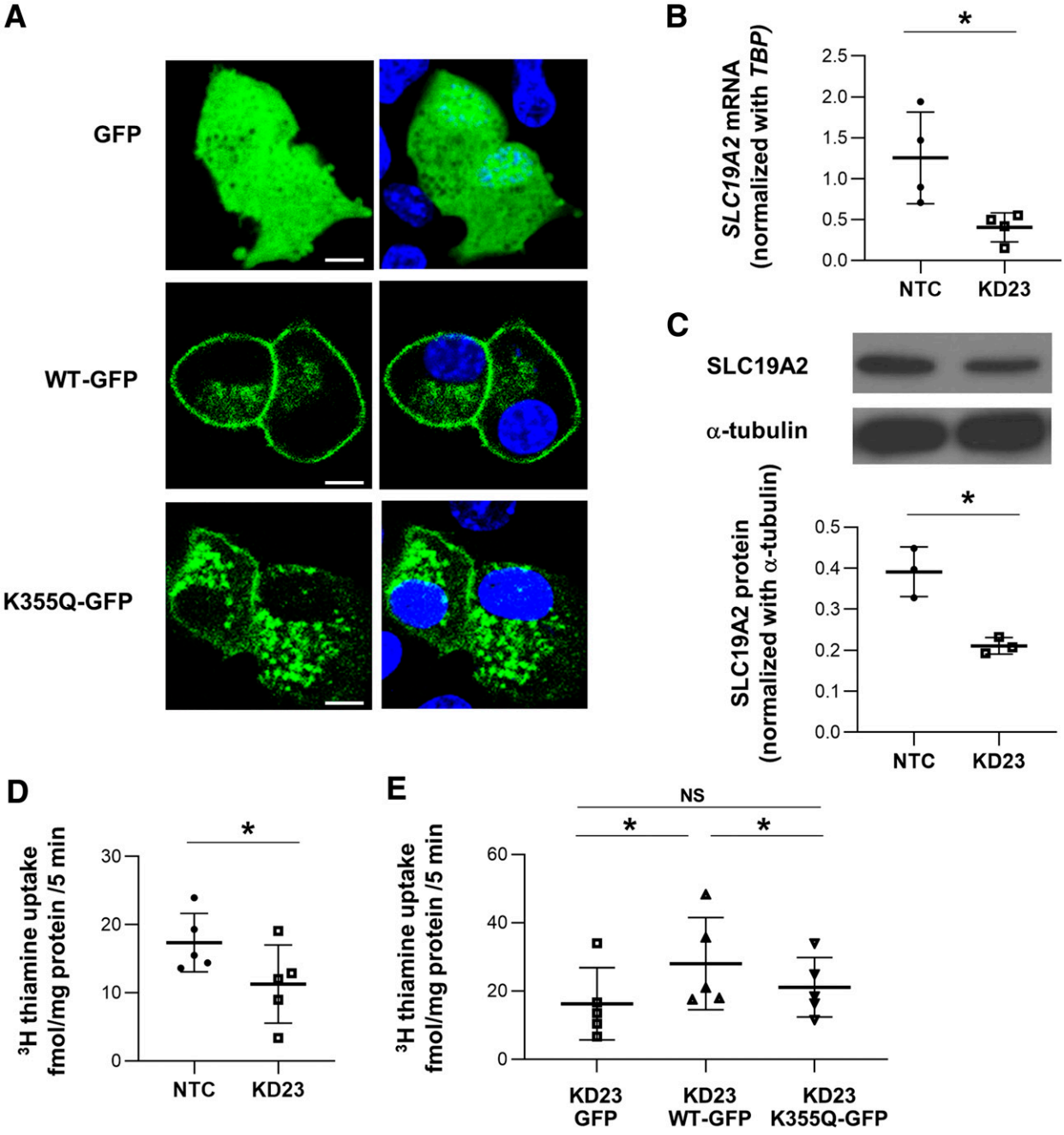

Figure 3—Retention of mutant SLC19A2 protein in cytoplasm is associated with loss of thiamine transporter function. *A*: Live cell imaging showing the phenotypes of GFP, SLC19A2-WT-GFP, and SLC19A2-K355Q-GFP (green) expressed in MIN6-m9 cells (left) with overlay of Hoechst 33258 (blue) staining for nucleus (right). Scale bars = 5 μm. Images are representative of three independent experiments. *B*: Quantitative RT-PCR analysis of *SLC19A2* mRNA levels in stable *SLC19A2* KD MIN6-m9 cells. Results were normalized to mouse TATA box binding protein (*TBP*) expression levels. Data are means ± SD of four independent experiments. *$P < 0.05$. *C*: Representative images and quantification of band intensity of Western blotting analysis of SLC19A2 and α-tubulin ($n = 3$). *D*: Uptake of [^{3}H]thiamine in KD23 MIN6-m9. Data are means ± SD. *$P < 0.05$. *E*: Retrieval of thiamine transporter function in KD23 MIN6-m9 by transient expression of SLC19A2-WT-GFP but not SLC19A2-K355Q-GFP. Data are means ± SD of five independent experiments. *$P < 0.05$. NS, not significant.

defective allele is associated with the development of diabetes accompanied by other clinical features that are related to the TRMA syndrome but are much milder and inconsistently present. We further show that the decreased thiamine uptake resulting from THTR1 deficiency may cause mitochondrial dysfunction, loss of protection against oxidative stress, and cell cycle arrest of β-cells, which may all contribute to the etiology of diabetes in *SLC19A2* mutation carriers, although a role of alterations in other tissues cannot be excluded given the high expression of *SLC19A2* in skeletal muscle, adipose tissue, thyroid, pituitary, and the adrenal cortex. Finally, we provide

Table 2—Relative *SLC19A2* and *SLC19A3* mRNA levels in MIN6-m9

Relative mRNA expression	NTC		KD23		
	Mean	SE	Mean	SE	*P*
SLC19A2/TBP	1.254307	0.280099	0.404448	0.088419	0.022206
SLC19A3/TBP	0.000765	0.000745	0.00196	0.000962	0.18

preliminary evidence suggesting that decreased THTR1 expression in β-cells, and perhaps other tissues, may be a feature of more common forms of diabetes and may possibly contribute to its pathogenesis, although no association with T2D has been identified to date by GWAS in the *SLC19A2* region.

Glucose intolerance in the absence of the full TRMA syndrome has previously been described in *SLC19A2* mutation heterozygous carriers from three TRMA families (15). Our findings confirm and expand that report by demonstrating segregation between an *SLC19A2* mutation and diabetes in an autosomal dominant fashion, albeit

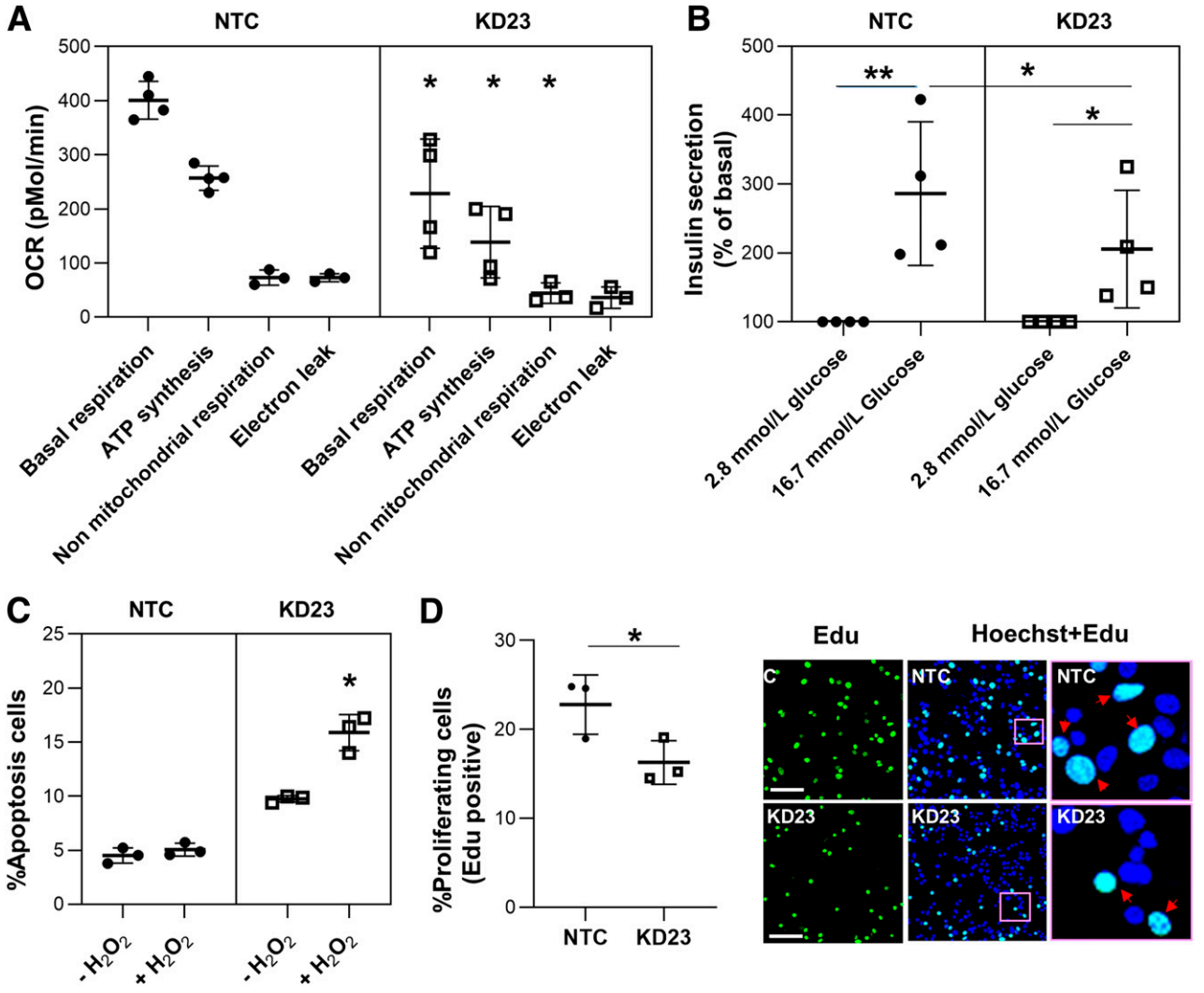

Figure 4—Mitochondrial respiration, response to glucose, and β-cell functions related to thiamine-dependent enzymes. *A*: Mitochondrial respiration profile of MIN6-m9 cells as measured by oxygen consumption rate (OCR). Data are means ± SD of four independent experiments. $^*P < 0.05$. *B*: Insulin released from MIN6-m9 under physiological and glucose-stimulated conditions. Data are means ± SD of four independent experiments. $^*P < 0.05$. $^{**}P < 0.0001$. *C*: Analysis of oxidative stress–induced apoptosis. Data are means ± SD of three independent experiments. $^*P < 0.05$. *D*: MIN6-m9 proliferation rate. Representative images of EdU (green) with overlay of Hoechst 33258 (blue) staining for nucleus. Pink boxes in the middle panels indicate areas shown at higher magnification in the right panels. Arrows indicate localizing of EdU and Hoechst. Scale bars = 50 μm. Data are means ± SD of three independent experiments. $^*P < 0.05$.

with incomplete penetrance. Autosomal dominant diabetes is a group of relatively rare genetically heterogeneous disorders, the best known of which is maturity-onset diabetes of the young (MODY)—a form of hyperglycemia characterized by an early onset, often before age 25 years, and an insulin secretion deficit (OMIM #606391). The average age at diagnosis in the family described in this report was 20 years, with three out of five affected carriers diagnosed before age 25 years and four out of five being treated with insulin. Given these clinical features, *SLC19A2* can probably be added to the list of MODY genes, which currently includes 14 loci (OMIM #606391). This form of MODY may not be limited to the family described in this article, as several *SLC19A2* damaging mutations (e.g., premature stop, frameshift), all rare (from 1 to 556 mutated alleles out of 121,320 chromosomes), can be found in the Exome Aggregation Consortium database.

The reason why diabetes, rather than other TRMA components, is the most prominent phenotype associated with heterozygosis for *SLC19A2* mutation remains unclear at this time. Intracellular thiamine levels are determined by the activities of two thiamine transporters, THTR1 and THTR2, which are coded by *SLC19A2* and *SLC19A3*, respectively (OMIM #603941 and #606152). Differences in the relative abundance of the two transporters may determine differences among tissues in the sensitivity to mutations in one or the other transporter. For instance, the expression of *SLC19A3* in pancreatic β-TC-6 cells, as well as in mouse and human primary pancreatic islets, was found to be significantly lower than that of *SLC19A2* (19). In addition, the capability of β-TC-6 cells to upregulate *SLC19A3* in response to thiamine depletion was limited compared with their ability to upregulate *SLC19A2* (19). Also, based on GTEx data, the expression of *SLC19A3* in the human pancreas seems to be much lower than that of *SLC19A2* (27). We also found suggestive evidence of lower expression of *SLC19A3* than *SLC19A2* in insulinoma MIN6-m9 cells, although a direct comparison between the two genes was not possible due to the different assays that were used for their measurement. After *SLC19A2* had been knocked down, we observed an increase in *SLC19A3* expression in these cells, but this was probably too small to offset the THTR1 deficiency caused by the *SLC19A2* KD. In other cell types, the expression of *SLC19A3* may be constitutionally higher or may increase more in response to THTR1 deficiency, thereby sparing these cells from the detrimental effects of *SLC19A2* mutations or thiamine deficiency. For instance, *SLC19A3* is the predominant thiamine transporter in intestinal epithelial cells where its expression, unlike that of *SLC19A2*, can be upregulated by thiamine deficiency (18). Interindividual variability in the THTR1-to-THTR2 ratio may also be responsible, along with differences in thiamine intake, for the variable clinical phenotype observed among *SLC19A2* mutation carriers.

Further complexity is provided by the existence of two alternatively spliced *SLC19A2* transcripts: a longer one (ENST00000236137) coding for the originally described 497 amino acid THTR1 protein and a shorter one (ENST00000367804) coding for a 296 amino acid isoform lacking amino acids 69–296. Since the p.Lys355Gln mutation is in a region shared by the two transcripts, and so was the target of the shRNA used for the functional experiments, one cannot say with certainty whether the phenotypes observed in the family and in the KD experiments are due to the deficit of one or the other isoform or both. The existence of two isoforms, which may be differentially impacted by the p.Lys355Gln mutation and whose relative expression may vary among individuals, may also explain some of the clinical heterogenity observed among mutation carriers.

On the mechanistic side, our findings confirm the well-known importance of mitochondrial function and ATP production for glucose sensing (28,29). The finding that intracellular thiamine deficiency has a significant impact on these processes and the suggestive evidence of lower *SLC19A2* expression in common forms of diabetes raise the possibility that supplementation with this vitamin may help prevent some forms of multifactorial type 2 diabetes. However, while this is a tantalizing hypothesis, much more evidence from in vitro and ex vivo studies is needed before clinical trials to test this intervention are planned.

In summary, this study describes a heterozygous mutation in the *SLC19A2* gene as the likely cause of an autosomal dominant form of diabetes with mild TRMA signs and provides preliminary evidence suggesting mitochondrial dysfunction, loss of protection against oxidative stress, and cell cycle arrest as potential mechanisms underlying impaired insulin secretion in *SLC19A2*-deficient β-cells. Further studies are needed to confirm the role of thiamine in the regulation of β-cell function and determine whether thiamine deficiency in β-cells may also contribute to more common forms of diabetes.

Acknowledgments. The authors thank all the subjects and families involved in the study. For more information, the following websites can be accessed: http://www.omim.org/, http://www.ncbi.nlm.nih.gov/RefSeq, http://www.ncbi.nlm.nih.gov/projects/SNP/, http://exac.broadinstitute.org, http://sift.jcvi.org, http://provean.jcvi.org/index.php, http://genetics.bwh.harvard.edu/pph2, http://www.mutationtaster.org, and http://mupro.proteomics.ics.uci.edu, and http://portals.broadinstitute.org/gpp/public/.

Funding. This work was supported by the National Institute of Diabetes and Digestive and Kidney Diseases, National Institutes of Health (grant R01DK55523 to R.N.K. and A.D., R01DK67536 to R.N.K., and P30DK36836 [Advanced Genomics and Genetics Core of the Diabetes Research Center at the Joslin Diabetes Center]); Thailand Research Fund IRG5980006; and the Faculty of Medicine of Siriraj Hospital, Mahidol University (Chalermphrakiat Grant and Research Fund R016034011 to P.J.). J.S. acknowledges grants for young researchers from Japan Association for Diabetes Education and Care and the support from Japan Diabetes Foundation. M.K.G. is supported by JDRF advanced postdoctoral fellowship grant 3-APF-2017-393-A-N.

Duality of Interest. No potential conflicts of interest relevant to this article were reported.

Author Contributions. P.J. conceived the idea, designed and performed experiments, analyzed the data, and wrote the manuscript. J.S. contributed to

experiments using primary islets of mouse and human. J.S. and C.C. conducted immunoblotting and immunostaining. P.B., A.P., T.H., and C.M. contributed genetic studies. M.K.G. conducted analyses using the Seahorse instrument. D.F.D.J. conducted glucose-stimulated insulin secretion assay. M.G.P. contributed to analysis of exome sequencing data. R.N.K. contributed to experimental design and discussion and edited the manuscript. A.D. conceived the idea; contributed to experimental design; analyzed the data; wrote, edited, and reviewed the manuscript; and contributed to discussions. All authors read and approved the manuscript. A.D. is the guarantor of this work and, as such, had full access to all the data in the study and takes responsibility for the integrity of the data and the accuracy of the data analysis.

Prior Presentation. Parts of this study were presented in abstract form at the 75th Scientific Sessions of the American Diabetes Association, Boston, MA, 5–9 June 2015.

References

1. Labay V, Raz T, Baron D, et al. Mutations in SLC19A2 cause thiamine-responsive megaloblastic anaemia associated with diabetes mellitus and deafness. Nat Genet 1999;22:300–304
2. Meire FM, Van Genderen MM, Lemmens K, Ens-Dokkum MH. Thiamine-responsive megaloblastic anemia syndrome (TRMA) with cone-rod dystrophy. Ophthalmic Genet 2000;21:243–250
3. Lorber A, Gazit AZ, Khoury A, Schwartz Y, Mandel H. Cardiac manifestations in thiamine-responsive megaloblastic anemia syndrome. Pediatr Cardiol 2003;24:476–481
4. Villa V, Rivellese A, Di Salle F, Iovine C, Poggi V, Capaldo B. Acute ischemic stroke in a young woman with the thiamine-responsive megaloblastic anemia syndrome. J Clin Endocrinol Metab 2000;85:947–949
5. Lagarde WH, Underwood LE, Moats-Staats BM, Calikoglu AS. Novel mutation in the SLC19A2 gene in an African-American female with thiamine-responsive megaloblastic anemia syndrome. Am J Med Genet A 2004;125A:299–305
6. Setoodeh A, Haghighi A, Saleh-Gohari N, Ellard S, Haghighi A. Identification of a SLC19A2 nonsense mutation in Persian families with thiamine-responsive megaloblastic anemia. Gene 2013;519:295–297
7. Scharfe C, Hauschild M, Klopstock T, et al. A novel mutation in the thiamine responsive megaloblastic anaemia gene SLC19A2 in a patient with deficiency of respiratory chain complex I. J Med Genet 2000;37:669–673
8. Abboud MR, Alexander D, Najjar SS. Diabetes mellitus, thiamine-dependent megaloblastic anemia, and sensorineural deafness associated with deficient alpha-ketoglutarate dehydrogenase activity. J Pediatr 1985;107:537–541
9. Pieczenik SR, Neustadt J. Mitochondrial dysfunction and molecular pathways of disease. Exp Mol Pathol 2007;83:84–92
10. Jha MK, Jeon S, Suk K. Pyruvate dehydrogenase kinases in the nervous system: their principal functions in neuronal-glial metabolic interaction and neurometabolic disorders. Curr Neuropharmacol 2012;10:393–403
11. Lax NZ, Gorman GS, Turnbull DM. Review: central nervous system involvement in mitochondrial disease. Neuropathol Appl Neurobiol 2017;43:102–118
12. Mandel H, Berant M, Hazani A, Naveh Y. Thiamine-dependent beriberi in the "thiamine-responsive anemia syndrome". N Engl J Med 1984;311:836–838
13. Poggi V, Longo G, DeVizia B, et al. Thiamin-responsive megaloblastic anaemia: a disorder of thiamin transport? J Inherit Metab Dis 1984;7(Suppl. 2):153–154
14. Oishi K, Diaz GA. Thiamine-responsive megaloblastic anemia syndrome. In GeneReviews. Pagon RA, Adam MP, Ardinger HH, et al., Eds. Seattle, WA, University of Washington, 1993
15. Neufeld EJ, Mandel H, Raz T, et al. Localization of the gene for thiamine-responsive megaloblastic anemia syndrome, on the long arm of chromosome 1, by homozygosity mapping. Am J Hum Genet 1997;61:1335–1341
16. Prudente S, Jungtrakoon P, Marucci A, et al. Loss-of-function mutations in APPL1 in familial diabetes mellitus. Am J Hum Genet 2015;97:177–185
17. Minami K, Yano H, Miki T, et al. Insulin secretion and differential gene expression in glucose-responsive and -unresponsive MIN6 sublines. Am J Physiol Endocrinol Metab 2000;279:E773–E781
18. Leibiger B, Moede T, Paschen M, et al. PI3K-C2α knockdown results in rerouting of insulin signaling and pancreatic beta cell proliferation. Cell Reports 2015;13:15–22
19. Mee L, Nabokina SM, Sekar VT, Subramanian VS, Maedler K, Said HM. Pancreatic beta cells and islets take up thiamin by a regulated carrier-mediated process: studies using mice and human pancreatic preparations. Am J Physiol Gastrointest Liver Physiol 2009;297:G197–G206
20. Ballinger SW, Shoffner JM, Hedaya EV, et al. Maternally transmitted diabetes and deafness associated with a 10.4 kb mitochondrial DNA deletion. Nat Genet 1992;1:11–15
21. Guillausseau PJ, Massin P, Dubois-LaForgue D, et al. Maternally inherited diabetes and deafness: a multicenter study. Ann Intern Med 2001;134:721–728
22. La Selva M, Beltramo E, Pagnozzi F, et al. Thiamine corrects delayed replication and decreases production of lactate and advanced glycation end-products in bovine retinal and human umbilical vein endothelial cells cultured under high glucose conditions. Diabetologia 1996;39:1263–1268
23. Hazell AS, Wang D, Oanea R, Sun S, Aghourian M, Yong JJ. Pyrithiamine-induced thiamine deficiency alters proliferation and neurogenesis in both neurogenic and vulnerable areas of the rat brain. Metab Brain Dis 2014;29:145–152
24. Shangari N, Bruce WR, Poon R, O'Brien PJ. Toxicity of glyoxals–role of oxidative stress, metabolic detoxification and thiamine deficiency. Biochem Soc Trans 2003;31:1390–1393
25. Sharma A, Bist R, Bubber P. Thiamine deficiency induces oxidative stress in brain mitochondria of Mus musculus. J Physiol Biochem 2013;69:539–546
26. Oishi K, Hofmann S, Diaz GA, et al. Targeted disruption of Slc19a2, the gene encoding the high-affinity thiamin transporter Thtr-1, causes diabetes mellitus, sensorineural deafness and megaloblastosis in mice. Hum Mol Genet 2002;11:2951–2960
27. Carithers LJ, Ardlie K, Barcus M, et al.; GTEx Consortium. A novel approach to high-quality postmortem tissue procurement: The GTEx Project. Biopreserv Biobank 2015;13:311–319
28. Detimary P, Gilon P, Nenquin M, Henquin JC. Two sites of glucose control of insulin release with distinct dependence on the energy state in pancreatic B-cells. Biochem J 1994;297:455–461
29. Pongratz RL, Kibbey RG, Kirkpatrick CL, et al. Mitochondrial dysfunction contributes to impaired insulin secretion in INS-1 cells with dominant-negative mutations of HNF-1alpha and in HNF-1alpha-deficient islets. J Biol Chem 2009;284:16808–16821